Interferometric measurement of refractive-index change in photosensitive glass

Tasshi Dennis, Erin M. Gill, and Sarah L. Gilbert

We report on a technique for determining the change in the refractive index of photosensitive glass. We have demonstrated our interferometer-based technique on fiber preform and bulk glass samples, achieving an optical-path-difference (OPD) repeatability of 0.2 nm. For the bulk glass sample we measured an OPD of 15.2 ± 3.0 nm, corresponding to an index change of $2.1 \pm 0.7 \times 10^{-5}$. Our technique was found to be insensitive to the effects of photodarkening and material compaction.

OCIS codes: 120.0120, 120.3180, 120.4530, 160.2290, 160.2750, 230.1480.

1. Introduction

Over the years, UV-induced index change in glass has been regarded as both a desirable phenomenon, as in the production of Bragg gratings and waveguide devices,[1] and an undesirable phenomenon, as in the degradation of photolithography optics.[2] Despite the development of numerous techniques to enhance or suppress it in various glass compositions, a fundamental understanding of the photosensitivity mechanism remains incomplete. For germanium-doped silica glass the primary mechanisms that have been proposed and studied are UV-induced defect centers that result in modified absorption[3,4] and material densification,[5] either of which may be accompanied by stress changes.[6] Although far from certain, it appears likely that a combination of the proposed mechanisms should be considered. Part of the difficulty in drawing firm conclusions from the studies arises from the wide array of glass compositions and process conditions involved and the limitations of the measurement techniques. In this paper we present an improved technique for the measurement of UV-induced index change in bulk glass samples.

In the fabrication of fiber Bragg gratings the induced index change is typically estimated from the device reflectivity with a coupled-mode analysis.[1] However, it would be useful if the index change could be determined without involving an optical fiber. A larger variety of glass compositions could be studied in the bulk form, and the dependence on glass composition could be distinguished from effects that are due to drawing-induced stress or defects. Interferometry has been used for index measurements of thin films[7] and optical fibers,[8] but there are few studies applicable to postirradiation measurements of bulk materials. Low-coherence interferometry is best suited to thickness and index-of-refraction measurements of thin films.[9] The most relevant studies have used commercial coherent interferometer systems to report on surface deformations that are due to compaction[10] as well as to measure the total optical path difference (OPD) through irradiated samples.[2] Our measurement technique uses small changes in a single interference fringe of a coherent Michelson interferometer to characterize the induced index change in bulk glass and fiber preform materials. By limiting the dynamic range of the measurement to a single interference fringe, periodically patterning the index change for averaging purposes, and designing custom digital signal processing, this technique achieves better absolute accuracy and repeatability than available instruments.

2. Experiment

Our technique for measuring induced index changes in photosensitive glass is based on observing the OPD that occurs when irradiated and unirradiated portions of a sample are passed through the arms of a Michelson interferometer. Figure 1 shows our measurement system, beginning with the beam from a single transverse-mode laser diode at 780 nm, which we shaped with an anamorphic prism pair and passed through an optical isolator. After spatial fil-

When this research was performed, the authors were with the Optoelectronics Division, National Institute of Standards and Technology, Boulder, Colorado 80305-3328. E. M. Gill is now with Datex-Ohmeda, Louisville, Colorado 80027-9560. T. Dennis's e-mail address is tasshi@boulder.nist.gov.

Received 22 August 2000; revised manuscript received 2 January 2001.

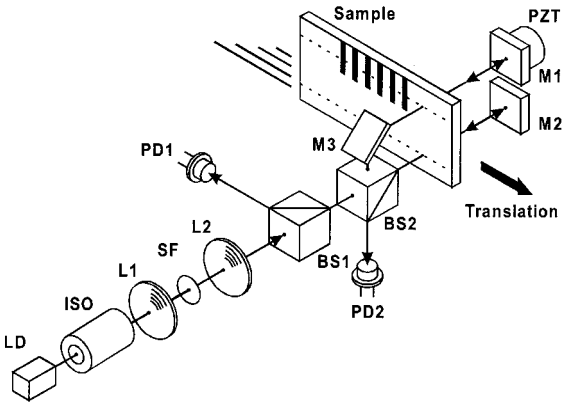

Fig. 1. Interferometric measurement system: LD, laser diode; ISO, optical isolator; L1 and L2, lenses; SF, spatial filter; BS1 and BS2, beam splitters; M1 and M2, return mirrors; M3, steering mirror; PZT, piezoelectric transducer; PD1 and PD2, photodiodes.

tering, we focused the beam through two beam splitters and the glass sample to be measured, producing a beam waist of ~30 μm on the return mirrors. The two output intensities of the interferometer exit the beam splitters as complementary functions of a phase that depends on the OPD and can be expressed as $I_1 \propto I_0(1 - \cos\phi)$ and $I_2 \propto I_0(1 + \cos\phi)$. Here I_0 is the input intensity and

$$\phi = 2\pi \frac{2(\mathrm{OPD})}{\lambda_{\mathrm{LD}}} \tag{1}$$

is the phase relationship between the interfering beams of the laser diode at vacuum wavelength λ_{LD} arising from the single-pass OPD. By individual detection of these intensities with gain-equalized photodiodes whose electrical signals are subtracted, a signal proportional to $I_0 \cos\phi$ is formed. This operation removes the dc component, creating a bipolar interferometric response that has multiple zero crossings, with linear slopes to a first-order approximation. The interferometer was locked onto one of the crossings (i.e., operated in quadrature) by use of the bipolar response to create the correction signal in a feedback loop. The signal was conditioned to compensate for drift and low-frequency noise and was applied to a piezoelectric transducer mounted behind mirror M1.

We prepared the samples by polishing a slab of the photosensitive glass and irradiating it with UV light in a periodic pattern over a portion of its area. The measurement system was designed so that both beams of the interferometer could simultaneously probe the sample, one through the pristine glass and the other through the periodically irradiated region, as shown in Fig. 1. The beams were separated vertically on the sample by a distance of ~3 mm. In this manner both beams sampled the larger-scale path-length changes caused by sample inhomogeneities and thickness variations, thereby canceling most of these effects. A spatial mapping of the OPD across the sample was produced by linear translation of the sample through the interferometer in the orientation shown. The periodicity of the UV-induced index change and the speed of the sample translation determine the frequency of the OPD signal. Thus a periodic waveform is generated by the interferometer while at the same time the finite gain of the feedback loop partially compensates for the periodic OPD change. The waveform can be observed on both the interferometer response and correction signal outputs; however, we found that the best signal-to-noise ratio (SNR) was achieved from the correction (feedback) signal.

Two different glass samples were prepared for analysis with our system: a bulk barium borosilicate crown glass with 5% by mole of germanium doping and a boro-germanosilicate fiber preform with a 7–10% by mole germanium-doped core. The bulk material was created in a glass melt, and the preform was grown by chemical deposition. A slice from the bulk sample ~4.5 mm thick was polished to a surface finish of λ/10 and a scratch–dig quality of 20/10 on both sides of 20 mm × 30 mm area. A 750-μm-wide amplitude mask was used for individual irradiation of six spots spaced 750 μm apart with 244-nm light from a frequency-doubled 488-nm continuous-wave (cw) argon-ion laser. On the basis of an average beam intensity of 5.1 W/cm^2 and an irradiation time of 50 min, we estimate the total fluence at each spot on the sample to be 15 kJ/cm^2. A thin section was cut from the preform, centered on and parallel to the core axis, exposing a photosensitive region 1.4 mm wide (the core diameter) and 3 cm long (the sample length), bordered on two sides by a 5-mm-wide cladding layer. The axial section provided a rectangular band of photosensitive material that was much larger than the circular area of a perpendicular slice. Both sides of the ~640-μm-thick section were polished to an estimated surface finish of λ/4. A KrF excimer laser at 248 nm and an amplitude mask with a series of slots 750 μm wide and spaced 750 μm apart was used to expose the band of core material. We deposited a total fluence of 5 kJ/cm^2, using 40 mJ/cm^2 pulses at a repetition rate of 200 Hz.

We removed the effect of surface defects incurred during the glass melt or preform deposition process by preparing samples from within the volume of the bulk and preform material. In the case of the preform, slicing through the core–cladding interface may have influenced the photosensitivity through stress relief. Differences in UV absorption between fiber and preform material, likely caused by drawing-induced defects or stress changes, have been documented.[3]

3. Results

Figure 2(a) shows a typical OPD mapping of the bulk sample produced by the interferometer and recorded with a digitizing oscilloscope. The homogeneity of the bulk glass resulted in high interferometric visibility and good SNR for the six UV-exposed regions. Most of the noise features have been correlated with motion of the translation stage. The slowly varying

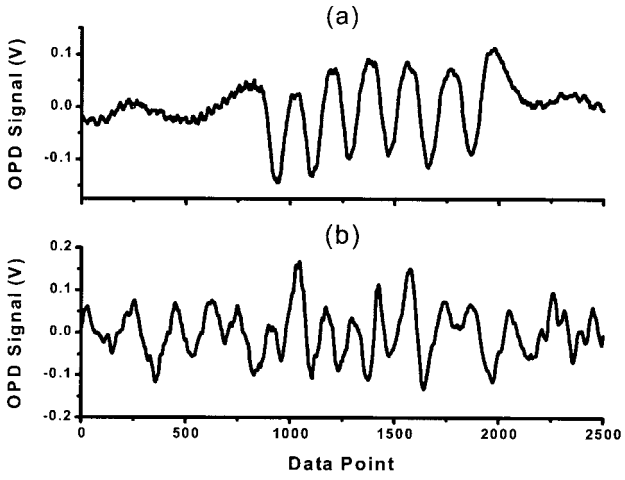

Fig. 2. Mappings of OPD's for (a) the bulk glass and (b) the preform as recorded with the interferometer. The OPD of the bulk glass was determined by use of all the waveform peaks, whereas the preform OPD used the central five peaks.

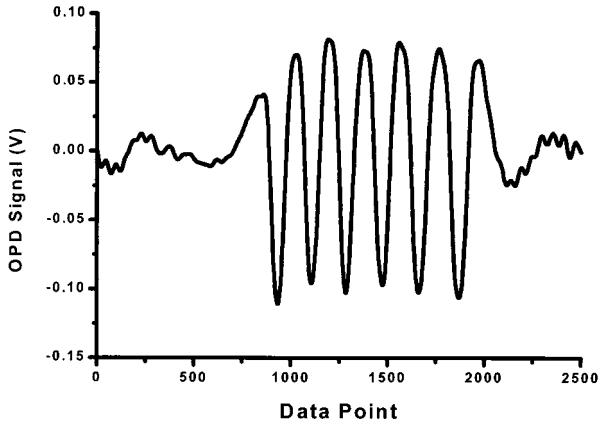

Fig. 3. Bulk glass OPD mapping after DSP has reduced the noise components caused primarily by motion of the translation stage.

ripple, beginning at a frequency below the OPD signal, was caused by irregular sample motion. Unfortunately, as the frequency of this noise increases, it becomes indistinguishable from the OPD signal. The high-frequency noise was caused primarily by motion of the translation stage that vibrated interferometer components, and it could be reduced by additional low-pass filtering.

Figure 2(b) shows a portion of a typical OPD mapping for the preform sample. A differentiator feedback circuit was incorporated to improve the noise performance at frequencies above the OPD signal. As compared with the bulk sample data, there is a greater amount of low-frequency noise, arising from the inhomogeneity of the sample: The center of the preform core has an index suppression of 50%, whereas the surrounding core material is fairly uniform with an index ripple of ~4%. The sample was carefully aligned to the focused interferometer beam so that the uniform region of the core was probed during axial translation. However, despite our best efforts, it is possible that portions of the beam strayed across and outside this region during translation, accounting for some of the slow baseline fluctuation. A sequence of five peaks near the center of the mapping was used in the data analysis.

Digital signal processing (DSP) was performed on the raw data to improve the SNR and to extract the average peak-to-peak amplitude of the OPD waveform. For the preform data we simply performed a baseline correction to remove the low-frequency noise component followed by peak-to-peak detection. To investigate the possibilities, a more sophisticated approach was taken with the bulk glass data. Finite-impulse-response digital filters, implementing a moving-average or nonrecursive algorithm, were designed to reject most of the translation stage noise. The high-frequency noise due to component vibration was easily removed with a low-pass filter having a cutoff at four times the signal frequency. The low-frequency ripple, however, resides in a narrow band in and between the signal and the lower-frequency component that defines the envelope of the waveform. The high-pass filter's cut-off frequency was chosen to preserve the average OPD amplitude of the raw data, and a single zero was placed in the stop band, centered between the signal and envelope components. Figure 3 shows the bulk glass signal of Fig. 2(a) after filtering, which reduces the standard deviation of the peak-to-peak amplitudes by more than a factor of 3.

By measuring the fringe visibility amplitude of the interferometer (the response $I_0 \cos \phi$ for a particular sample), we could express the average peak-to-peak voltage amplitude of the waveform as an OPD in units of nanometers. Because the OPD is small compared with the measurement wavelength, the interferometer's response at a zero crossing can be considered linear, with a slope equal to one-half the peak-to-peak amplitude of the visibility pattern divided by a unit radian. A second calibration factor accounts for the attenuation of the measured waveform amplitude that is due to the feedback circuit and low-pass filtering. This compensation is necessary, since the fringe visibility amplitude was measured without feedback and filtering, owing to its having a higher frequency than the OPD waveform. These factors combine to allow the measured waveform amplitude to be expressed as a change in phase ϕ, which is proportional to the OPD through Eq. (1). Through this procedure we obtained average OPD values of 15.2 nm from 10 mappings of the bulk glass and 17.4 nm from 15 mappings of the fiber preform.

We performed an uncertainty analysis on the bulk glass data to validate the OPD determination and to indicate the utility of the technique for future studies of photosensitivity. The analysis helps to identify the areas of technical refinement that would allow this technique to reach its potential for higher absolute accuracy. The major sources of uncertainty are summarized in Table 1. We measured the emission wavelength of the interferometer's laser diode to be 784.9 nm, using an optical spectrum analyzer

Table 1. Example Uncertainty Budget for OPD Determination

Source of Uncertainty	Standard Uncertainty (1σ) (in nm)
Source wavelength accuracy and stability	0.01
Relative voltage measurement	0.9
Calibration uncertainty	1.1
Noise after DSP	0.5
Combined standard uncertainty (RSS)	1.5

(0.5-nm absolute uncertainty), and observed a linewidth and stability sufficient to consider it to be monochromatic. A substantial uncertainty was introduced during the voltage measurement of the OPD mapping and the fringe-visibility pattern. An oscilloscope is generally not an accurate measurement device, and because the OPD amplitude was a factor of 30 smaller than the calibration signal, different gain settings were required.

The calibration of the interferometric system had the greatest uncertainty, mainly because the responses with and without feedback had to be correlated accurately, as already stated. An uncertainty was introduced in the process of combining the measured frequency response of the interferometer, feedback circuit, and low-pass filter at the frequency of the OPD signal. In addition, there was an uncertainty due to the spread in frequency of the OPD signal, which was likely caused by nonlinear sample motion and a nonsinusoidal irradiation pattern. Finally, the basic measurement equipment used during calibration introduced uncertainties that could be estimated from the manufacturer's specifications. The value presented in Table 1 is a root-sum-of-squares (RSS) combination of these factors.

The standard deviation due to noise before DSP was 1.3 nm, as calculated from the SNR of the raw data. The majority of the noise was caused by mechanical vibration that was due to sample translation. Other contributors were the spot-to-spot variation in optical fluence deposited during UV exposure, the electrical amplifier noise, the surface quality and finish, and the amplitude noise of the laser. The noise uncertainty of 0.5 nm shown in Table 1 is the standard deviation of the individual peak-to-peak amplitudes of the OPD after DSP has been applied. The combined standard uncertainty of 1.5 nm for the OPD measurement is a RSS combination of the Table 1 entries. Thus we conclude that the OPD for the bulk sample is 15.2 ± 3.0 nm, where our quoted uncertainty is the expanded uncertainty with a coverage factor of 2 (i.e., our value is $\pm 2\sigma$).

The repeatability of our technique was estimated from multiple OPD measurements of a single index step of the bulk glass sample. Analysis of only one feature removed the effects of the spot-to-spot variation in optical fluence deposited during UV exposure and the noise signature of the translation stage. The standard deviation of the measurements yields a repeatability of 0.2 nm (1σ).

To interpret the average OPD values in terms of an index change, we needed to estimate the depth of the photosensitive response. This is difficult to quantify, since the index profile most likely follows an exponential decay into the sample, influenced by saturation effects. Our method has been to use the depth at which the absorption of UV radiation reaches the $1/e$ value, ignoring saturation. Samples of the bulk and preform material were prepared in a manner identical to those measured by the interferometer, only with much smaller thickness to increase the UV transmission. We measured the absorption depth of the bulk glass, using a 250-μm-thick sample and a scanning UV-visible spectrometer. The absorption depth was calculated on the basis of an exponential decay model with compensation for Fresnel reflections from the front and back surfaces. At the irradiation wavelength of 244 nm, we measured an absorption coefficient of $\alpha = 1.39 \pm 0.38\ \mathrm{mm}^{-1}$, corresponding to a $1/e$ depth of 717 ± 200 μm (2σ). The preform measurements proved to be much more challenging because of a much higher material absorption. Using the 244-nm cw laser source, different from the 248-nm pulsed KrF laser used for sample processing, we measured a very large value of $\alpha \approx 68\ \mathrm{mm}^{-1}$ in a 150-μm-thick sample, corresponding to a $1/e$ depth of only ~15 μm. With these values we interpret the bulk and preform OPD's as index changes of $2.1 \pm 0.7 \times 10^{-5}$ and roughly 1.2×10^{-3}, respectively.

The irradiated regions of both samples were scanned with a mechanical-stylus profilometer for surface deformations that could have been caused by material compaction. The bulk glass showed no signs of surface structure down to the 1-nm level, although a periodic darkening identical to the irradiation pattern was evident in the material volume. The presence of both this solarization effect and an index change in the infrared would appear to conflict with the results of a previous study of photosensitive fiber.[8] However, we note that our results were obtained from a bulk material with a different composition that had been made with a different fabrication process. For the purpose of evaluating our measurement technique we estimate that the darkening was responsible for a reduction of 1.8% in transmission intensity at 780 nm, causing an underestimate of the OPD of less than 1%. In contrast to the bulk glass, the photosensitive core region of the preform exhibited a distinct square-wave surface structure with a 1.5-mm period, matching that of the amplitude mask pattern used during irradiation. The average depth of these features was 27 nm, observed over several periods. We estimated the index change due to compaction, using a differential form of the Lorentz–Lorenz relationship,[11]

$$\Delta n = \frac{(n^2 - 1)(n^2 + 2)}{6n} \frac{\Delta t}{t}. \tag{2}$$

In this expression n is the refractive index (1.47) of the preform core, t is the thickness (640 μm) of the sample, and Δt is the depth (27 nm) of the surface deformation. With these values we calculated an average index change of 2.3×10^{-5}, effective over the entire sample thickness t. Because the effects of compaction (reduced sample thickness and increased refractive index) tend to cancel each other in an OPD measurement, the observed compaction accounts for only 2 nm of the 17.4-nm measured OPD. For this reason we conclude that our measurement technique is not very sensitive to this photosensitivity mechanism. Because we are interested only in the contribution specific to our experiment, our volumetric analysis did not take into consideration any constraining effects of the surrounding pristine material on the index change.

4. Conclusion

We have demonstrated an interferometric technique for measuring the total induced index change in photosensitive bulk glass and fiber preform materials. In the case of the bulk glass, an index change of $2.1 \pm 0.7 \times 10^{-5}$ was measured without any sign of compaction, yet it displayed color features indicative of solarization. By contrast, a portion of the much larger 1.2×10^{-3} index change observed in the preform glass could be attributed to material compaction, with no sign of solarization. The material properties were observed in the process of evaluating our measurement technique, and the fact that only two samples were involved prevents us from making general conclusions about the mechanisms of photosensitivity. Our technique appears to be insensitive to the solarization effect, which is advantageous, but it is also somewhat insensitive to compaction, owing to the offsetting effects of reduced sample thickness and increased refractive index. For the bulk glass measurement, our analysis shows that we achieved a combined absolute uncertainty of 3.0 nm (2σ) and a repeatability of 0.2 nm (1σ). Both these figures demonstrate a performance that is better than that of commercial systems with which we are familiar. Our technique achieves this by limiting the dynamic range of the measurement to a single interference fringe, periodically patterning the index change for averaging purposes, and designing custom digital signal processing (DSP) for each glass sample. Despite this success, we expect that our performance could easily be improved through technical refinements. Of particular importance would be a better OPD calibration technique, perhaps one involving a calibration standard with known thickness variations and constant index. The uncertainty and the repeatability could easily be reduced with a more accurate means of acquiring the voltage waveforms; a high-resolution data-acquisition board is one possibility. A more smoothly running translation stage, perhaps one designed with air bearings, could dramatically improve the SNR while reducing the need for DSP. Conceptually, a better model for the depth of the index change, one that accounts for the material saturation that is due to incident light, is needed, especially for absolute measurements. The measurement technique we have presented should enable more-detailed investigations in future studies of photosensitivity, particularly ones that involve relative comparisons of a material subjected to varying process conditions.

We thank J. Hayden and S. Pucilowski (Schott Glass Technologies, Inc.) for providing the bulk glass and A. Carter (Redfern Fibres, Inc.) for providing the preform used in this study.

References

1. A. Othonos, "Fiber Bragg gratings," Rev. Sci. Instrum. **68,** 4309–4341 (1997).
2. R. Schenker, P. Schermerhorn, and W. G. Oldham, "Deep-ultraviolet damage to fused silica," J. Vac. Sci. Technol. B **12,** 3275–3279 (1994).
3. D. L. Williams, S. T. Davey, R. Kashyap, J. R. Armitage, and B. J. Ainslie, "Ultraviolet absorption studies on photosensitive germanosilicate preforms and fibers," Appl. Phys. Lett. **59,** 762–764 (1991).
4. R. M. Atkins, V. Mizrahi, and T. Erdogan, "248 nm induced vacuum UV spectral changes in optical fibre preform cores: support for a colour centre model of photosensitivity," Electron. Lett. **28,** 385–387 (1993).
5. M. Douay, W. X. Xie, T. Taunay, P. Bernage, P. Niay, P. Cordier, B. Poumellec, L. Dong, J. F. Bayon, H. Poignant, and E. Delevaque, "Densification involved in the UV-based photosensitivity of silica glasses and optical fibers," J. Lightwave Technol. **15,** 1329–1342 (1997).
6. M. G. Sceats, G. R. Atkins, and S. B. Poole, "Photolytic index changes in optical fibers," Annu. Rev. Mater. Sci. **23,** 381–410 (1993).
7. T. Fukano and I. Yamaguchi, "Simultaneous measurement of thicknesses and refractive indices of multiple layers by a low-coherence confocal interference microscope," Opt. Lett. **21,** 1942–1944 (1996).
8. J. Canning, A. L. G. Carter, and M. G. Sceats, "Correlation between photodarkening and index change during 193 nm irradiation of germanosilicate and phosphosilicate fibers," J. Lightwave Technol. **15,** 1348–1356 (1997).
9. P. A. Flournoy, R. W. McClure, and G. Wyntjes, "White-light interferometric thickness gauge," Appl. Opt. **11,** 1907–1915 (1972).
10. N. F. Borrelli, D. C. Allan, and R. A. Modavis, "Direct measurement of 248- and 193-nm excimer-induced densification in silica-germania waveguide blanks," J. Opt. Soc. Am. B **16,** 1672–1679 (1999).
11. M. Born and E. Wolf, *Principles of Optics*, 6th ed. (Pergamon, New York, 1980), p. 87.